



Dimensionality and irreversibility of field-induced transitions in SrDy₂O₄

C. Bidaud,¹ O. Simard,¹ G. Quirion,^{1,2} B. Prévost,³ S. Daneau,³ A. D. Bianchi,³ H. A. Dabkowska,⁴ and J. A. Quilliam^{1,*}

¹*Département de Physique, Université de Sherbrooke, Sherbrooke, Québec, Canada J1K 2R1*

²*Department of Physics and Physical Oceanography, Memorial University, St. John's, Newfoundland, Canada A1B 3X7*

³*Département de Physique, Université de Montréal, Montréal, Québec, Canada H3T 1J4*

⁴*Brockhouse Institute for Materials Research, McMaster University, Hamilton, Ontario, Canada L8S 4M1*

(Received 15 October 2015; revised manuscript received 22 January 2016; published 12 February 2016)

Low-temperature ultrasound velocity measurements are presented on the frustrated spin system SrDy₂O₄ that allow us to define high-resolution phase diagrams with the magnetic field applied along all three principal axes. For $H||b$, a region of field-induced long-range order is delimited by a dome of first-order phase transitions. An unusual magnetization process is observed with significant irreversibility at very low temperatures when passing between the low-field spin liquid phase and the long-range ordered phase which we attribute to large energy barriers. For $H||c$, the system appears to remain effectively one dimensional, exhibiting two transitions as a function of magnetic field, but no finite-temperature long-range order.

DOI: [10.1103/PhysRevB.93.060404](https://doi.org/10.1103/PhysRevB.93.060404)

An attractive feature of rare-earth magnets is the possibility to grow isostructural materials with many different ions, each with distinct total angular momentum and anisotropy, providing a wealth of diverse physical phenomena for a given lattice. While the pyrochlores are undoubtedly the best studied set of isostructural rare-earth materials [1], a new group of materials with the formula AR_2O_4 has recently become a popular field of study [2]. The A ion can be either Sr or Ba and the rare-earth ion is highly flexible, with Ho [3], Dy [4], Er [5], and Yb [6] having recently been studied. When viewed along the c axis, these materials have a honeycomb structure (see Fig. 1). However, from the point of view of interactions, they are likely best represented by a model of two inequivalent sets of frustrated zigzag spin chains with weaker interchain coupling [2].

One of the most intriguing materials in this class is SrDy₂O₄ which, in zero field, shows no indications of long-range order (LRO) down to low temperatures, suggesting a possible spin liquid ground state [7]. In magnetic fields, however, thermodynamic measurements show evidence of order [4,8]. In particular, with $H||b$, the magnetization appears to show a plateau from 0.5 to 1.5 T at roughly 1/3 of the partially saturated moment, suggesting that an up-up-down ($\uparrow\uparrow\downarrow$) state is stabilized by quantum fluctuations [8]. Inelastic neutron scattering measurements and crystal field calculations [3] have allowed for a determination of crystal field levels in SrDy₂O₄, and indicate that the easy axis of site 1 (the red chains) is the c direction whereas the easy axis of site 2 (the blue chains) is in the ab plane and is nearly parallel to the b axis (see Fig. 1). Based on bond lengths in the zigzag chains, they may be well described by a frustrated one-dimensional (1D) anisotropic next-nearest-neighbor Ising (ANNNI) model [9].

In this Rapid Communication we present a study of the phase diagram of SrDy₂O₄ using ultrasound velocity measurements down to low temperatures, an order of magnitude below what was previously obtained in thermodynamic

measurements. The sound velocity shows precise anomalies at magnetic phase transitions, providing a high-resolution phase diagram. Notably, we find that the effective dimensionality of the system (with respect to magnetic degrees of freedom) depends heavily on the direction of the applied magnetic field. We have also carefully studied the effect of field history, making it possible to identify first-order phase transitions, glassy dynamics, and strong irreversibility when passing between spin liquid and ordered phases.

A single crystal of SrDy₂O₄, grown by the floating zone technique, was cut with faces perpendicular to the orthorhombic axes a , b , and c ($2.26 \times 2.36 \times 2.30$ mm³). Transverse piezoelectric transducers were glued on opposite faces of the crystal, oriented such that shear waves were propagated along the c axis (along the chains) with polarization in the a direction. An ultrasonic interferometer was used to measure the velocity of the first elastic transmitted pulse (at 92 MHz), which is proportional to the elastic constant C_{55} . The absolute velocity is found by time of flight to be 1440 ± 15 m/s. The sample was cooled in a dilution refrigerator and the field was applied along the a , b , or c axes. Relative changes in velocity, $\Delta v/v$, primarily reflect changes in the restoring forces due to magnetoelastic coupling, providing a sensitive probe of the magnetization and magnetic order parameters [10,11]. Magnetoelastic coupling often results from modulation of the exchange interaction between spins, though in rare-earth materials it may also come from modulation of the crystal field [12]. The C_{44} elastic constant was also measured on a different sample of SrDy₂O₄ and gave essentially the same results, although with overall larger variations.

$H||b$ (*blue chains/Dy2*). We begin with a discussion of the richest phase diagram, that is, for $H||b$, where the field is primarily influencing the spins on the blue chains (Dy2). Anomalies in the sound velocity are primarily associated with changes in the square of the magnetization M_{2b}^2 , the development of an order parameter S^2 , and low-frequency spin fluctuations. Relative changes in velocity are shown as a function of magnetic field in Fig. 2(a). Below ~ 1.5 K, we typically observe three separate anomalies where the slope of $v(B)$ changes sign.

*jeffrey.quilliam@usherbrooke.ca

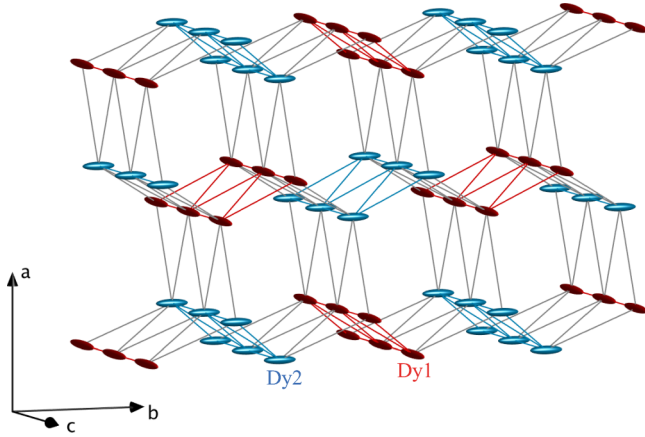


FIG. 1. Structure of Dy ions in SrDy_2O_4 , with the shape of the ellipsoids illustrating the easy axes of the two sites. Site Dy1 (red) has its easy axis along c and site Dy2 (blue) has its easy axis along b .

The first two critical fields, H_{b1} and H_{b2} , are found to converge as the temperature is raised, forming a dome, inside of which is likely a LRO magnetic state. Hysteresis loops indicate that the dome of LRO is delimited by first-order transitions. This can be seen in the field scans in Fig. 2(a), where solid (dotted) lines indicate increasing (decreasing) field, and in the temperature scans of Fig. 2(b). As a function of temperature the lattice is found to soften at the transition (i.e., the velocity is reduced), indicating a negative coupling to the square of the order parameter S^2 . Hence, in the phase diagram of Fig. 3(c), we have used a minimum in $\partial v/\partial H$ to signal the onset of the order parameter at H_{b1} and the maximum of $\partial v/\partial H$ to signal the disappearance of the order parameter at H_{b2} . Given that

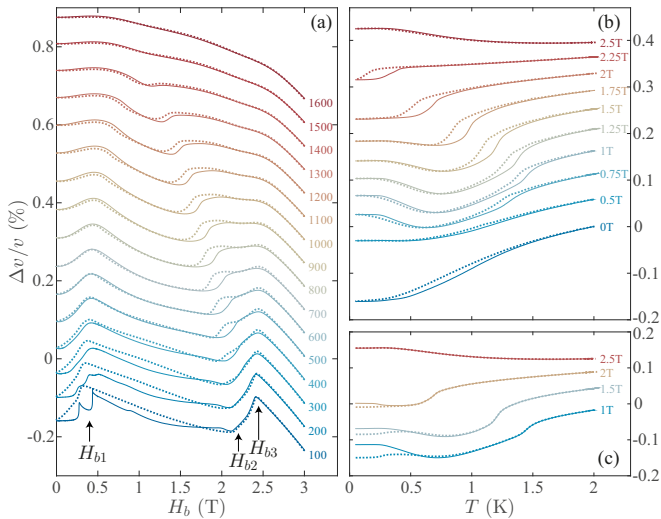


FIG. 2. (a) Relative change in sound velocity as a function of $H||b$. Dotted lines are for decreasing field, and solid lines are for increasing field. Temperatures labels are given in units of mK. (b) Relative change in sound velocity as a function of T for various fields $H||b$. Dotted lines are for FC and solid lines are for FCW. (c) Temperature scans of $\Delta v/v$ for $H||b$ showing the difference between FCW (solid lines) and ZFCW (dotted lines). Curves have been staggered for ease of viewing.

the magnetization is close to 1/3 of the saturated value in the region under the dome shown in Fig. 3 [8], this may be an $\uparrow\uparrow\downarrow$ phase on chains formed by Dy2 ions with an easy axis anisotropy pointing along the b axis (see the blue chains in Fig. 1). Such a plateau can be seen in simulations of the frustrated 1D ANNNI model thought to apply to this material [13].

Although we associate anomalies at H_{b1} and H_{b2} with true phase transitions, the origin of the maximum observed in the sound velocity at around $H_{b3} \simeq 2.5$ T seems quite different [Fig. 2(a)] in that it is quickly smeared out with increasing temperature. Consequently, we attribute this maximum to a crossover at which the blue chain spins reach their full polarization, as shown in magnetization data for $H||b$ [8]. Despite full polarization of Dy2 (blue chains) above H_{b3} , we nonetheless observe that $\Delta v/v \propto -H_b^2$. In order to account for this significant field dependence of the velocity above H_{b3} , we must invoke a negative magnetoelastic coupling with spins on the other chain (red chain/Dy1), which in this regime continue to show a small magnetization that is linear in magnetic field, as measured in Ref. [8]. The leading-order field dependence of the velocity of transverse acoustic waves then simply reduces to $\Delta v/v = kM_{1b}^2 = k\chi_{1b}^2 H^2$ [11], where k is a coupling constant (either related to exchange striction or modulation of crystal fields) and χ_{1b} is the constant magnetic susceptibility of spins on the red chains (Dy1) with the field along the b axis.

This material's phase diagram shows several regions of hysteresis with a complex field-history dependence. We have therefore performed temperature scans using three different protocols: (1) cooling in field (FC), (2) warming after field cooling (FCW), and (3) warming after zero-field cooling (ZFCW). The FC and FCW curves primarily show the hysteresis associated with supercooling at the first-order transition, as shown in Fig. 2(b). In Fig. 2(c), we instead observe a strong difference between FCW and ZFCW curves only below ~ 500 mK. It seems that cooling the sample in the liquid phase at zero field locks in a significant level of disorder. On increasing the field into the LRO phase, some disorder remains frozen in, probably in the form of domains.

Strangely, below ~ 250 mK, the transition at H_{b2} [Fig. 2(a)] no longer shows hysteresis and the same anomalies are seen in both cooling and warming curves. The values of critical fields in this region therefore become somewhat ambiguous. The most peculiar behavior is seen in the field-history dependence of the low-temperature phase transition at H_{b1} which becomes very complex below ~ 300 mK. For decreasing magnetic field only one anomaly is observed at 0.36 T (we define the transition as the minimum in $\partial v/\partial H$). However, for increasing magnetic field, H_{b1} appears to bifurcate into three separate anomalies which, at 100 mK, are found at 0.27, 0.44, and 0.91 T. This is evident in the surface plot of Fig. 3(a), where we show $(\partial v/\partial H)/v$, as well as in the phase diagram presented in Fig. 3(c).

This unusual irreversibility can be likely explained by the slow dynamics that are observed at low field, for example, as a FC-ZFC splitting in magnetization measurements [8]. We also find a difference between cooling and warming curves which indicates slow dynamics in the liquid phase, but this difference depends on the sweep rate and does not show a pronounced dip in velocity at a specific temperature, as is expected for a spin glass transition [14]. Likely, this system can best be described

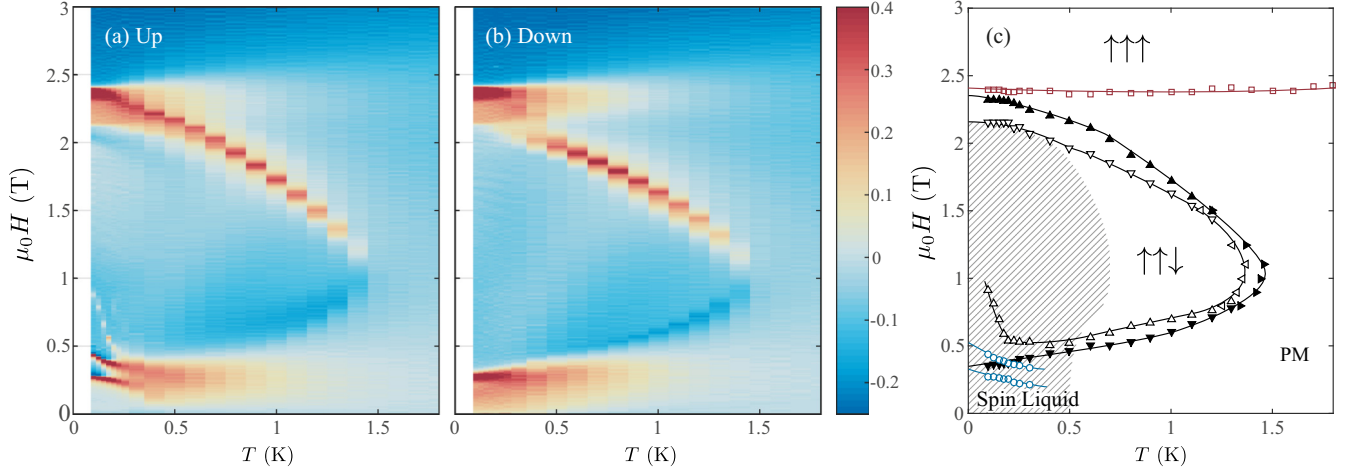


FIG. 3. Surface plots of the field derivative of sound velocity $(\partial v/\partial H)/v$ as a function of H_b and temperature for (a) increasing field and (b) decreasing field. In addition to a shift of the position of the dome of LRO (due to hysteresis at the first-order phase transitions), the “up” curves demonstrate a great deal of increased structure in the vicinity of H_{b1} , with this line of transitions appearing to bifurcate into three separate transitions. (c) Phase diagram for $H||b$. Blue circles are the two initial jumps seen when raising the magnetic field. Black triangles present the first-order phase transitions that delimit what is likely the $\uparrow\uparrow\downarrow$ LRO phase, with the orientation of the triangles indicating the direction of field or temperature sweeps. Red squares illustrate the crossover to full polarization (of Dy2). The hatched region roughly shows where slow (glassy) dynamics is observed.

as a “classical” spin liquid, with slow dynamics and minimal quantum fluctuations.

Similar to spin ice, SrDy_2O_4 in zero field may progressively freeze into one of many possible degenerate disordered ground states with relatively short-range correlations. Many rare-earth Ising systems similar to this one can even manifest extremely slow spin dynamics in paramagnetic [15,16] and spin liquid [17,18] phases due to very small quantum tunneling matrix elements, although this is not universally true (see, for instance, Ref. [19]). When the magnetic field is increased, one selects a particular ground state (likely an $\uparrow\uparrow\downarrow$ state), but the transition from the disordered liquid state to LRO is a violent one as significant energy barriers must be overcome in order to reconfigure small domains into extended order. This transition is evidently achieved in three distinct steps. Only once the field reaches close to 1 T, much higher than the 0.5 T transition that is measured at slightly higher temperatures, is the system finally able to achieve LRO. Even then, a domain structure must persist, as evidenced by the significant difference between ZFCW and FCW curves in Fig. 1(c). On the other hand, when decreasing the magnetic field across H_{b1} , the transition is able to proceed much more smoothly as the $\uparrow\uparrow\downarrow$ configuration may be much closer to one of the many possible, short-range ordered ground states permissible in the spin liquid phase, and in this case a single anomaly is observed. Fennell *et al.* [3] have demonstrated one-dimensional, short-range, $\uparrow\uparrow\downarrow$ correlations in this phase, and it would be useful to explore theoretically how the system passes between such a short-range ordered state and $\uparrow\uparrow\downarrow$ order.

Strong irreversibility in field sweeps has also been observed in spin ice, the most famous example of a classical spin liquid. Specifically, with the field along the [111] direction, a strong irreversibility was seen well below any phase transitions with magnetization [20], ultrasound velocity [21], and thermal conductivity [22] measurements. Again, significant

energy barriers, in this case connected to hopping magnetic monopoles [23,24], make it difficult to increase the level of order in the system, leading to avalanches and irreversibility.

$H||c$ (red chains/Dy1). The relative sound velocity is shown as a function of $H||c$ in Fig. 4(a). These field sweeps show qualitatively similar behavior to those with $H||b$ including

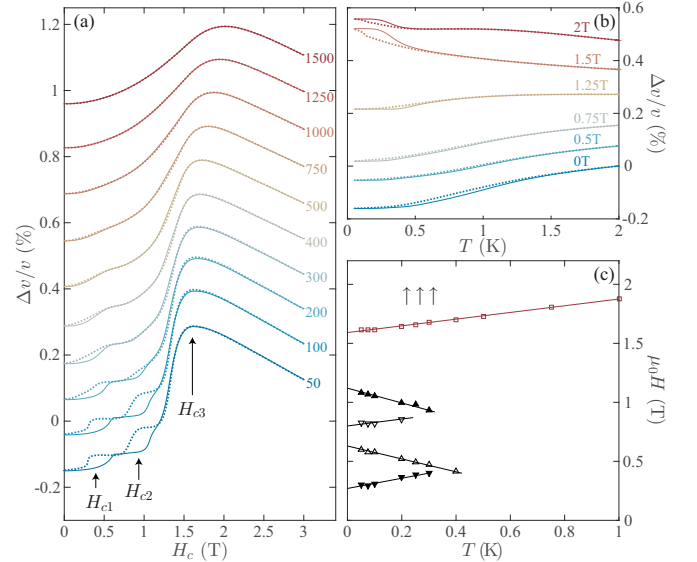


FIG. 4. Relative change in sound velocity for $H||c$ (a) as a function field and (b) as a function of temperature. Solid lines correspond to increasing field or temperature and dotted lines correspond to decreasing field or temperature. Curves have been staggered for ease of viewing. (c) Phase diagram for $H||c$. The orientation of the triangles indicates the direction of the field sweeps. The red squares show a crossover to a ferromagnetic (fully polarized) phase.

two hysteretic anomalies and a maximum in the velocity. Quantitatively speaking, these transitions occur at lower field values: $H_{c1} = 0.295$ (0.595) T and $H_{c2} = 0.821$ (1.07) T for decreasing (increasing) fields at 50 mK. Saturation of the red chain magnetization gives a very pronounced maximum at $H_{c3} \simeq 1.3$ T, as opposed to $H_{b3} \simeq 2.4$ T. Above this point we again have a negative H^2 background. In this case, we speculate that the background comes from the uniform magnetization of Dy2, M_{2c} , which should be roughly linear for this field direction.

With increasing temperature, the H_{c1} and H_{c2} anomalies disappear much more quickly than their counterparts for $H||b$. The striking difference in the $H||c$ data is the lack of phase transitions as a function of temperature. In other words, there does not appear to be a dome of LRO for $H||c$. In particular, this can be seen in the temperature sweep at 0.75 T in Fig. 4(b) (in between the critical fields) which is quite featureless. Thus it appears that the Dy1 sites (red chains) never develop true LRO at a finite temperature, although they may be approaching a zero-temperature LRO, consistent with an anisotropic 1D system. It appears that due to some details of the system's Hamiltonian, the effective dimensionality of this material varies with field direction. Clear three-dimensional LRO is found when $H||b$, but the system remains effectively one dimensional when $H||c$.

It is important to highlight the fact that significant slow (glassy) dynamics persists below 500 mK for essentially all values of magnetic field when $H||c$. This glassiness becomes particularly evident above 1.5 T, as can be seen in the hysteresis loops in Fig. 4, but this progressive spin freezing does not develop at a sharp glass transition. This is a point that deserves further research with other techniques such as ac susceptibility or muon spin rotation (μ SR), which are better suited to studying slow spin dynamics.

$H||a$. When the magnetic field is applied in the a direction, the obtained curves are relatively featureless, as shown in the Supplemental Material [25], apart from some weak hysteresis at the lowest temperatures. $\Delta v/v$ initially increases as H_a^2 , indicating a quadratic coupling to a linear $M_a(H_a)$. This is not surprising given that the a direction is a hard axis for both types of spin. Some leveling off (beginning of saturation) is noticed by 3 T, as is the case in the magnetization data [8].

There is a degree of similarity between this material and others in the SrLn_2O_4 family in that one often encounters very different physics on the two different rare-earth sites [26]. With the exception of SrYb_2O_4 [6], LRO occurs on at most one of the rare-earth sites in all members of this family of materials [27]. In SrHo_2O_4 the red chains appear to develop fairly conventional long-range Néel order ($\uparrow\downarrow\uparrow\downarrow$) whereas the blue chains develop only short-range order with ($\uparrow\uparrow\downarrow\downarrow$) correlations [28]. Wen *et al.* [28] have argued that in SrHo_2O_4 ,

a larger crystal field energy for site 2 (blue chains) leads to slower dynamics and causes them to be quenched into a disordered state. This same logic evidently does not apply to SrDy_2O_4 , however, which only seems to show LRO on the blue chains (the site that presumably has slower dynamics) under applied field $H||b$. The coexistence of LRO and SRO has also been observed in SrEr_2O_4 [5], BaNd_2O_4 [29], and SrTb_2O_4 [30]. Two other systems in the family, BaTb_2O_4 [27] and SrTm_2O_4 [31], do not show any magnetic order in zero field.

In conclusion, this work has elaborated detailed phase diagrams of SrDy_2O_4 for magnetic fields along the b and c directions [Figs. 3(c) and 4(c)]. Our results are consistent with those of magnetization [8] and specific heat [4] measurements, but extend to lower temperatures and provide much higher resolution. Whereas a clear dome of long-range order is found for $H||b$ for spins with a b -axis anisotropy (blue chains), the red chains appear to remain disordered for all magnetic fields, with LRO only possibly occurring in the zero-temperature limit when $H||c$. This suggests a difference in effective dimensionality depending on the direction in which the magnetic field is applied.

Finally, we have shown that there is no ordering anomaly in zero field down to 50 mK, therefore providing strong evidence of frustration and a likely spin liquid ground state, whereas previous thermodynamic measurements have only reached ~ 500 mK [4,8]. Slow dynamics suggests a “classical” spin liquid with only short-range correlations [3] along with large energy barriers and a progressive slowing of spin dynamics, similar to spin ice, for example [17]. A very strong irreversibility at the first critical field value seems to be consistent with a transition into or out of a classical spin liquid with large energy barriers impeding ordering of the spins as the field is increased. It remains to be seen whether the origin of the spin liquid phase and the unusual transitions to LRO can be understood within the context of 1D ANNNI models or whether additional complications such as the long-range dipolar interaction, interchain couplings, and additional crystal field levels are essential to modeling the magnetism in SrDy_2O_4 . Further measurements aiming to better understand the microscopic model of this material (especially the crystal field scheme) should undoubtedly be carried out in order to help provide a theoretical description of the interesting emergent physics observed in this work.

We are grateful to M. Castonguay for extensive technical support, and we acknowledge valuable discussions with M. Kenzelmann, M. Gingras, and A. Aczel. This work was supported by NSERC and the RQMP, which is funded by the Fonds de recherche du Québec - Nature et technologies (FRQNT).

-
- [1] J. S. Gardner, M. J. P. Gingras, and J. E. Greedan, *Rev. Mod. Phys.* **82**, 53 (2010).
 [2] O. A. Petrenko, *Low Temp. Phys.* **40**, 106 (2014).
 [3] A. Fennell, V. Y. Pomjakushin, A. Uldry, B. Delley, B. Prévost, A. Désilets-Benoit, A. D. Bianchi, R. I. Bewley, B. R. Hansen,

T. Klimczuk, R. J. Cava, and M. Kenzelmann, *Phys. Rev. B* **89**, 224511 (2014).

- [4] T. H. Cheffings, M. R. Lees, G. Balakrishnan, and O. A. Petrenko, *J. Phys.: Condens. Matter* **25**, 256001 (2013).

- [5] T. J. Hayes, G. Balakrishnan, P. P. Deen, P. Manuel, L. C. Chapon, and O. A. Petrenko, *Phys. Rev. B* **84**, 174435 (2011).
- [6] D. L. Quintero-Castro, B. Lake, M. Reehuis, A. Niazi, H. Ryll, A. T. M. N. Islam, T. Fennell, S. A. J. Kimber, B. Klemke, J. Ollivier, V. G. Sakai, P. P. Deen, and H. Mutka, *Phys. Rev. B* **86**, 064203 (2012).
- [7] L. Balents, *Nature (London)* **464**, 199 (2010).
- [8] T. J. Hayes, O. Young, G. Balakrishnan, and O. A. Petrenko, *J. Phys. Soc. Jpn.* **81**, 024708 (2012).
- [9] W. Selke, *Phys. Rep.* **170**, 213 (1988).
- [10] G. Quirion, T. Taylor, and M. Poirier, *Phys. Rev. B* **72**, 094403 (2005).
- [11] G. Quirion, X. Han, M. L. Plumer, and M. Poirier, *Phys. Rev. Lett.* **97**, 077202 (2006).
- [12] B. Lüthi, *Physical Acoustics in the Solid State* (Springer, Berlin, 2005).
- [13] T. H. Yang, W. S. Lin, X. T. Jia, M. H. Qin, and J. M. Liu, *Physica A* **410**, 253 (2014).
- [14] F. S. Huang, *J. Appl. Phys.* **54**, 5718 (1983).
- [15] J. A. Quilliam, S. Meng, and J. B. Kycia, *Phys. Rev. B* **85**, 184415 (2012).
- [16] M. Schechter and P. C. E. Stamp, *Phys. Rev. B* **78**, 054438 (2008).
- [17] J. Snyder, J. S. Slusky, R. J. Cava, and P. Schiffer, *Nature (London)* **413**, 48 (2001).
- [18] J. A. Quilliam, L. R. Yaraskavitch, H. A. Dabkowska, B. D. Gaulin, and J. B. Kycia, *Phys. Rev. B* **83**, 094424 (2011).
- [19] J. G. Rau and M. J. P. Gingras, *Phys. Rev. B* **92**, 144417 (2015).
- [20] D. Slobinsky, C. Castelnovo, R. A. Borzi, A. S. Gibbs, A. P. Mackenzie, R. Moessner, and S. A. Grigera, *Phys. Rev. Lett.* **105**, 267205 (2010).
- [21] S. Erfanfiam, S. Zherlitsyn, J. Wosnitza, R. Moessner, O. A. Petrenko, G. Balakrishnan, and A. A. Zvyagin, *Phys. Rev. B* **84**, 220404(R) (2011).
- [22] C. Fan, Z. Y. Zhao, H. D. Zhou, X. M. Wang, Q. J. Li, F. B. Zhang, X. Zhao, and X. F. Sun, *Phys. Rev. B* **87**, 144404 (2013).
- [23] C. Castelnovo, R. Moessner, and S. L. Sondhi, *Nature (London)* **451**, 42 (2008).
- [24] L. D. C. Jaubert and P. C. W. Holdsworth, *Nat. Phys.* **5**, 258 (2009).
- [25] See Supplemental Material at <http://link.aps.org/supplemental/10.1103/PhysRevB.93.060404> for data taken with the magnetic field parallel to the a direction.
- [26] O. Young, A. R. Wildes, P. Manuel, B. Ouladdiaf, D. D. Khalyavin, G. Balakrishnan, and O. A. Petrenko, *Phys. Rev. B* **88**, 024411 (2013).
- [27] A. A. Aczel, L. Li, V. O. Garlea, J.-Q. Yan, F. Weickert, V. S. Zapf, R. Movshovich, M. Jaime, P. J. Baker, V. Keppens, and D. Mandrus, *Phys. Rev. B* **92**, 041110(R) (2015).
- [28] J. J. Wen, W. Tian, V. O. Garlea, S. M. Koohpayeh, T. M. McQueen, H.-F. Li, J.-Q. Yan, J. A. Rodriguez-Rivera, D. Vaknin, and C. L. Broholm, *Phys. Rev. B* **91**, 054424 (2015).
- [29] A. A. Aczel, L. Li, V. O. Garlea, J.-Q. Yan, F. Weickert, M. Jaime, B. Maiorov, R. Movshovich, L. Civale, V. Keppens, and D. Mandrus, *Phys. Rev. B* **90**, 134403 (2014).
- [30] H. F. Li, C. Zhang, A. Senyshyn, A. Wildes, K. Schmalzl, W. Schmidt, M. Boehm, E. Ressouche, B. Hou, P. Meuffels, G. Roth, and T. Brückel, *Front. Phys.* **2**, 42 (2014).
- [31] H.-F. Li, A. Senyshyn, O. Fabelo, J. Persson, B. Hou, M. Boehm, K. Schmalzl, W. Schmidt, J.-P. Vassalli, P. Thakuria, X. Sun, L. Wang, G. Khazaradze, B. Schmitz, C. Zhang, G. Roth, J. G. Rocah, and A. Wildes, *J. Mater. Chem. C*, **3**, 7658 (2015).